Superionic behaviour in copper(I) chloride at high pressures and high temperatures

1996 J. Phys.: Condens. Matter 8 6191

(http://iopscience.iop.org/0953-8984/8/34/009)

J. Phys.: Condens. Matter **8** (1996) 6191–6198. Printed in the UK

Superionic behaviour in copper(I) chloride at high pressures and high temperatures

S Hull and D A Keen

ISIS Science Division (Diffraction), Rutherford Appleton Laboratory, Chilton, Didcot OX11 0QX, UK

Received 12 March 1996, in final form 28 May 1996

Abstract. Neutron powder diffraction studies of copper(I) chloride have been performed at pressures to 7.3 kbar and temperatures to 740 K. The presence of a solid phase at pressures greater than ∼2 kbar and temperatures greater than ∼700 K, identified in previous differential thermal analysis studies, is confirmed. This phase, labelled CuCl-III, has a cubic structure, space group $I\bar{4}3m$. The chlorine anions form a body-centred cubic sublattice and the copper cations are randomly distributed over the 12(d) tetrahedral sites at $(\frac{1}{4}, 0, \frac{1}{2})$ etc. Both the basic structure and the nature of the thermally induced disorder appear similar to those shown by the ambient pressure superionic phases α-AgI and α-CuBr. As a result, CuCl can no longer be considered an anomalous (non-superionic) member of the family of binary, tetrahedrally coordinated halide compounds.

1. Introduction

The three copper(I) halides CuCl, CuBr and CuI all adopt the cubic zinc-blende structure at ambient conditions (γ-phases) and AgI usually exists as a mixture of the zinc-blende phase (γ-AgI) and the hexagonal equivalent wurtzite structure (β-AgI) [1]. As summarized in table 1, all four compounds undergo structural phase transitions on increasing temperature. The three β-phases of the copper halides (β-CuCl, β-CuBr and β-CuI) all have the wurtzite or related structures [5–8]. These phases exhibit relatively high values of ionic conductivity ($\sigma \sim 0.01$–$0.1\ \Omega^{-1}\text{cm}^{-1}$ [9]) and powder neutron diffraction studies indicate that the cations undergo large and anharmonic thermal vibrations [5–8]. However, the cations remain predominantly on the regular lattice positions with only limited occupation of interstitial sites. In contrast, complete disorder of the cation sublattice is characteristic of the three α-phases (α-AgI, α-CuBr and α-CuI). These are true superionic phases and possess very high ionic conductivities ($\sigma \sim 0.1$–$1\ \Omega^{-1}\text{cm}^{-1}$) which are comparable to the molten state [9]. Powder neutron diffraction has shown that the superionic phases comprise an essentially rigid anion sublattice, which is body-centred cubic (b.c.c.) in α-AgI [3, 4] and α-CuBr [6, 7] and face-centred cubic (f.c.c.) in α-CuI [6]. The smaller cations (Ag^+ or Cu^+) then undergo rapid hops between interstitial voids formed by the anion sublattice. In the case of α-AgI, the work of Wright and Fender [3] and Nield *et al* [5] suggests that the cations predominantly hop between tetrahedral interstices via the trigonal sites, with little or no occupation of the octahedral cavities (see figure 1).

It is clear from the above that copper(I) chloride differs from AgI, CuBr and CuI because it does not adopt a superionic phase with complete cation disorder on increasing temperature at ambient pressure. The pressure–temperature phase diagram of CuCl is shown

0953-8984/96/346191+08$19.50

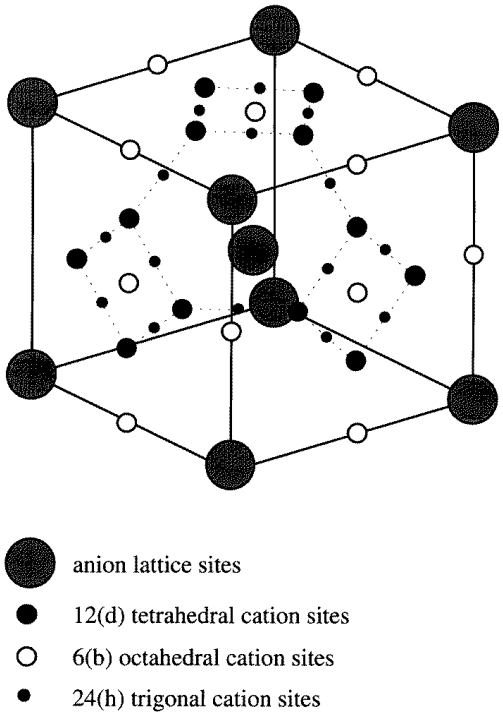

Figure 1. A schematic diagram of the unit cell of a superionic phase with a body-centred cubic (b.c.c.) anion sublattice (after Wright and Fender [3]). The various interstitial sites which the cations may populate are illustrated. The dotted lines show the conduction paths between tetrahedral sites via trigonal sites.

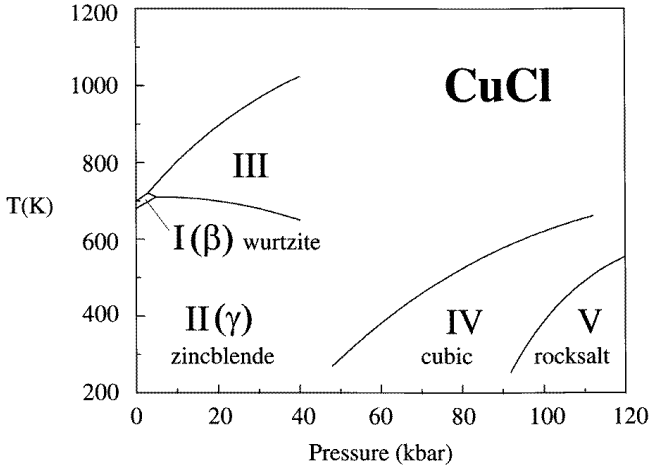

Figure 2. The pressure–temperature phase diagram of CuCl, taken from Merrill [2].

in figure 2, taken from the review by Merrill [2]. In the earliest studies of CuCl at elevated pressures and temperatures, Jayaraman *et al* [10] used differential thermal analysis (D.T.A.)

Table 1. A summary of the temperature-induced phase transitions in the four tetrahedrally coordinated halide compounds. The conventional notation for the various phases (γ, β, α) is given together with that used by Merrill [2] to describe the pressure–temperature phase diagrams. Phases denoted by the symbol # exhibit limited cation disorder and those denoted by * are true superionic phases, in which the cations are randomly distributed over a larger number of available sites.

Compound	Phase	T-range (K)	Structure	Space group	Reference
AgI	γ II′	$0 \rightarrow 420$	Zinc-blende	$F\bar{4}3m$	[1]
	$\beta^{\#}$ II	$0 \rightarrow 420$	Wurtzite	$P\bar{6}_3mc$	[1]
	α^{*} I	$420 \rightarrow 829$	b.c.c. I^- sublattice	$Im\bar{3}m$	[3, 4]
CuCl	γ II	$0 \rightarrow 681$	Zinc-blende	$F\bar{4}3m$	[1]
	$\beta^{\#}$ I	$681 \rightarrow 703$	Wurtzite	$P\bar{6}_3mc$	[5]
CuBr	γ III	$0 \rightarrow 664$	Zinc-blende	$F\bar{4}3m$	[1]
	$\beta^{\#}$ II	$664 \rightarrow 744$	Wurtzite	$P\bar{6}_3mc$	[6 ,7]
	α^{*} I	$744 \rightarrow 765$	b.c.c. Br^- sublattice	$Im\bar{3}m$	[6, 7]
CuI	γ III	$0 \rightarrow 642$	Zinc-blende	$F\bar{4}3m$	[1]
	$\beta^{\#}$ II	$642 \rightarrow 680$	Hexagonal	$P\bar{3}m1$	[6, 8]
	α^{*} I	$680 \rightarrow 878$	f.c.c. I^- sublattice	$Fm3m$	[6]

to map the melting curve to ∼40 kbar. Subsequent measurements by Rapoport and Pistorius using the same technique [11] observed a second, weaker transition at higher temperatures. This was identified as the real melting curve, with the original boundary reassigned to a solid → solid transition with the resultant new phase labelled CuCl-III. The later assignment seems plausible, because the melting temperature of CuCl then increases with pressure in the same manner as those of CuBr and CuI [11]. This paper describes the first diffraction studies of CuCl at elevated temperatures and pressures, including structural investigation of the phase CuCl-III.

2. Experimental details

The diffraction studies were performed on the Polaris powder diffractometer [12] at the ISIS spallation neutron source, UK, using zinc sulphide scintillator detectors situated at scattering angles in the range $85^\circ < \pm 2\theta < 95^\circ$. These collect diffraction data using the time-of-flight method over the d-spacing range from ∼0.3 Å to ∼4.3 Å with essentially constant $\Delta d/d$ resolution of ∼0.6%. Commercially available CuCl powder supplied by the Aldrich Chemical Co., of stated purity 99.995+%, was used in these measurements. The powdered sample material was compressed into a copper capsule 8 mm in diameter and 25 mm in length. All operations were performed in an argon atmosphere because CuCl is known to be sensitive to moist air. Details of the heatable pressure cell used for these experiments will be given in a forthcoming paper [13].

Time-of-flight Rietveld refinements of the powder diffraction data used the computer programme TF12LS [14]. In assessing the relative quality of fits to the experimental data using different structural models the usual χ^2-statistic is used, defined by

$$\chi^2 = \sum_{N_d} \frac{(I_{obs} - I_{calc})^2}{(\sigma I_{obs})^2} \Big/ (N_d - N_p). \tag{1}$$

N_d is the number of data points used in the fit and N_p is the number of fitted parameters. I_{obs}

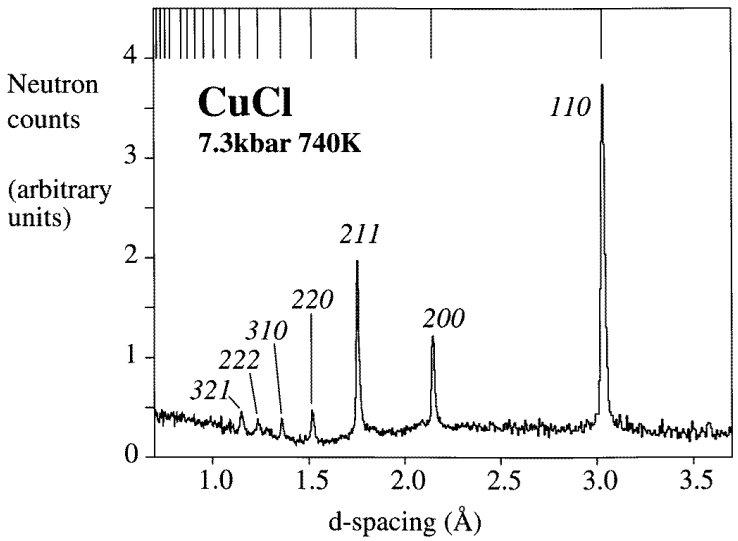

Figure 3. Diffraction data from phase CuCl-III collected at 7.3 kbar and 740 K. The tick marks along the top of the figure illustrate the calculated positions of Bragg peaks from a body-centred cubic lattice with $a = 4.30$ Å, with the *hkl*-values shown.

and I_{calc} are the observed and calculated intensities, respectively, and σI_{obs} is the estimated standard deviation on I_{obs}, derived from the counting statistics.

3. Results

The sample was initially compressed at ambient temperature and the pressure determined to be 7.3(1) kbar using the measured lattice parameter of the zinc-blende-structured γ-phase and the bulk modulus of CuCl ($B_0 = 381 \pm 6$ kbar [15]). Relatively rapid diffraction measurements were made at temperatures of 380 K, 500 K, 620 K and 740 K. The latter showed a dramatic change in the diffraction pattern with new, though significantly weaker, Bragg peaks at d-spacings of ∼1.75 Å, ∼2.15 Å and ∼3.05 Å. No evidence of peaks arising from remaining zinc-blende phase could be observed, indicating complete transformation to a new phase. With reference to the p–T phase diagram (figure 2), this is clearly the phase CuCl-III and a long data collection run (∼14 hours) was performed under these conditions. The resultant diffraction pattern, following the subtraction of scattering measured with an empty cell, is illustrated in figure 3. Seven Bragg peaks could be clearly identified, with d-spacings consistent with a body-centred cubic lattice, of lattice parameter $a \sim 4.30$ Å.

The observed diffraction pattern shows evidence of extensive disorder within phase CuCl-III. The rapid fall-off in Bragg peak intensity with decreasing d-spacing is evidence of large thermal vibrations and the diffuse scattering, observed as undulations in the background in figure 3, arises from short-range correlations between disordered ions. The diffuse scattering seen in figure 3 is qualitatively the same as that observed in superionic α-AgI [4]. Unfortunately, detailed analysis of the diffuse scattering [4, 7] is not possible with the current data because the geometry of the pressure cell limits the angular range over which the scattering can be measured [13]. As a result, the diffuse scattering contribution was estimated in the regions of d-spacings between the Bragg peaks, interpolated over the whole

Table 2. A summary of the fits to the diffraction data collected at 7.3 kbar and 740 K using models A to E, described in the text. χ^2 is the goodness-of-fit statistic defined in equation (1).

Model	Description	χ^2
A	b.c.c. anion sublattice, no cations	4.66
B	b.c.c. anion sublattice, cations in 6(b) octahedral sites	2.94
C	b.c.c. anion sublattice, cations in 12(d) tetrahedral sites	2.20
D	b.c.c. anion sublattice, cations in 24(h) trigonal sites	2.50
E	b.c.c. anion sublattice, cations in 12(d) and 24(h) sites	2.12

Table 3. Summary of the structural parameters of phase CuCl-III measured in this work.

CuCl phase III	
Pressure	$p = 7.3(1)$ kbar
Temperature	$T = 740(3)$ K
Space group	$Im\bar{3}m$
Lattice parameter	$a = 4.3011(6)$ Å
Cl^- positions	2(a) sites @ $(0,0,0)$, $(\frac{1}{2}, \frac{1}{2}, \frac{1}{2})$
Cl^- isotropic thermal parameter	$B_{Cl} = 4.7(2)$ Å^2
Cu^+ positions	12(d) sites @ $(\frac{1}{4}, \frac{1}{2}, 0)$ etc
Cu^+ isotropic thermal parameter	$B_{Cu} = 10.3(6)$ Å^2

pattern and then subtracted.

We begin by placing Cl^- in the 2(a) positions at (0, 0, 0) and $(\frac{1}{2}, \frac{1}{2}, \frac{1}{2})$ in space group $Im\bar{3}m$, forming a body-centred sublattice of the type found in α-AgI [3, 4] and α-CuBr [6, 7]. Attempts to fit the data with this physically unrealistic model resulted in only a modest fit to the data, with $\chi^2 = 4.66$ (see table 2). To locate the cations we first consider three alternative models, labelled B, C and D, which distribute the Cu^+ randomly over all the available octahedral, tetrahedral and trigonal interstices, respectively. The octahedral 6(b) sites are located at $(\frac{1}{2}, \frac{1}{2}, 0)$ etc, the tetrahedral 12(d) sites at $(\frac{1}{4}, \frac{1}{2}, 0)$ etc and the trigonal 24(h) sites at $(x, x, 0)$ etc. with $x = \frac{3}{8}$. These sites are illustrated in figure 1 and the results of fits to the diffraction data using each model are listed in table 2. Attempts to locate the cations in octahedral sites (model B) do not provide a good fit to the experimental data. In addition, these result in anomalously small values for the cation thermal vibration parameter and this model must be discounted. Model C produces a slightly better fit than model D indicating that tetrahedral sites are predominantly occupied, as in the case of α-AgI [3, 4] and α-CuBr [6, 7]. Model E, which allows the cations to be distributed over both tetrahedral and trigonal sites, produces a small improvement to the fit with a ratio of tetrahedral to trigonal occupancies of ~3:1. However, model E increases the number of fitted structural variables and excessive correlations between the fitted values of cation occupancy and thermal parameters occur. Recalling the relatively small number of measured Bragg peaks, model E cannot be considered a statistically significant improvement over model C. The final fitted parameters, obtained using model C, are listed in table 3. Figure 4 illustrates the quality of the fit to the experimental data using this model.

The relatively large values of the isotropic thermal vibration parameters of Cu^+ given in table 3 ($B_{Cu} = 10.3(6)$ Å^2) are indicative of considerable disorder. It is probable that the cation thermal vibrations are anisotropic and/or anharmonic, depending on the site symmetry. However, attempts to model the thermal vibrations using these more complex descriptions

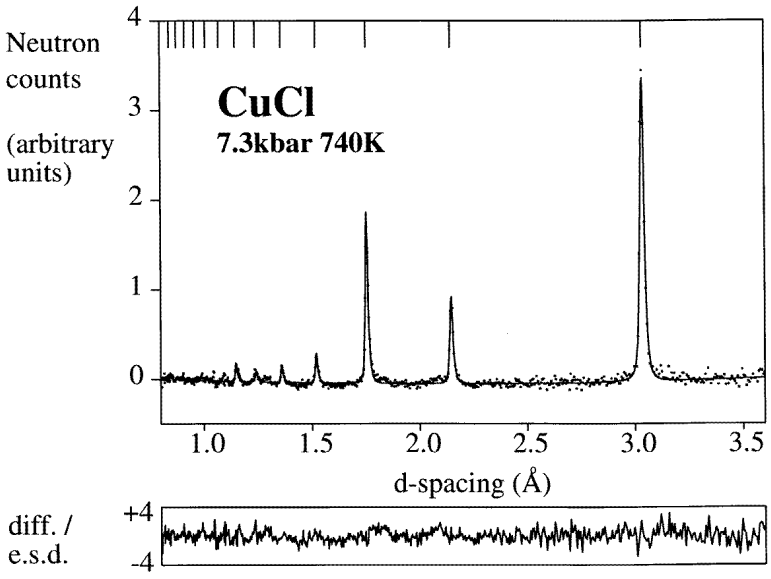

Figure 4. Least-squares refinement of the diffraction data from CuCl-III collected at 7.3 kbar and 740 K. The dots are the experimental points and the solid line is the profile calculated using the structural model described in table 3. The tick marks at the top of the upper plot show the calculated positions of the Bragg peaks and the lower trace shows the difference (measured minus calculated) divided by the estimated standard deviation on the points.

did not significantly improve the quality of the fit, despite the inclusion of additional fitted parameters. In particular, it was not possible to model any anharmonic behaviour of the cations in the tetrahedral sites at $(\frac{1}{4}, \frac{1}{2}, 0)$ by 'splitting' these into $\frac{1}{12}$-occupied 24(g) sites at $(x, \frac{1}{2}, 0)$ and $(\frac{1}{2}, -x, 0)$ etc with $x \sim 0.30$ (as discussed for the case of α-AgI by Wright and Fender [3]) or into to $\frac{1}{24}$-occupied 48(i) sites at $(\frac{1}{4}, \frac{1}{2} - x, x)$, $(\frac{1}{4}, \frac{1}{2} + x, -x)$, $(\frac{1}{4}, \frac{1}{2} + x, x)$ and $(\frac{1}{4}, \frac{1}{2} - x, -x)$ etc with $x \neq 0$.

Following the data collection at 740 K the sample was cooled at the same pressure of 7.3 kbar to determine the transition temperature between phases III and II (γ-CuCl). At a temperature of 710(3) K coexistence of these two solid phases was observed. On further cooling to 700(3) K all of the diffraction peaks from CuCl-III disappeared. The transition temperature is in good agreement with the D.T.A. study of Rapoport and Pistorius [11]. The unit-cell volumes per CuCl formula unit, obtained from the data set with both CuCl-III and CuCl-II present, are 39.73(2) Å^3 and 39.63(1) Å^3, respectively. CuCl-III is, therefore, only marginally less dense than CuCl-II ($\sim$0.25%), as might be expected from the near-horizontal phase boundary shown in the p–T phase diagram (figure 2).

4. Discussion

The structural model for phase CuCl-III derived in the previous section is qualitatively similar to that of the superionic phases α-AgI [3, 4] and α-CuBr [6, 7]. However, the conclusion that CuCl-III is a superionic phase requires some caution. It should be emphasized that measurements of the Bragg diffraction determine the *time-averaged* structure and cannot directly differentiate between static and dynamic disorder. Evidence

for the superionic nature of phase CuCl-III is contained in the original D.T.A. work of Rapoport and Pistorius [11] because the signal at the II $\rightarrow$ III transition was noted as being larger than that at the III $\rightarrow$ liquid one. In the harmonic approximation, the mean thermal displacement $\bar{u}$ of the cation away from the centre of the tetrahedral void is given by $B = 8\pi u^{-2}$. Using $B_{Cu} = 10.3(6)$ Å^2 (table 3), this gives a value $\bar{u} \sim 0.65$ Å which is almost half the distance $a/\sqrt{8} \sim 1.5$ Å between the tetrahedral interstices. As a result, significant overlap of the scattering density from each tetrahedral site will occur at the 24(h) sites and migration of cations through these trigonal sites will take place in ⟨110⟩ directions. The presence of this overlap explains the difficulties described above in attempting to fit a structural model (E) which includes discrete occupancy of the trigonal sites.

No measurements of the ionic conductivity of CuCl in the region of p–T space around CuCl-III have been reported to date. However, the factors discussed above provide compelling evidence that phase CuCl-III is superionic. As a consequence, CuCl can no longer be considered anomalous with respect to the three other tetrahedrally coordinated compounds. In the structural model for the superionic phases (figure 1) the cations diffuse through the polyhedral faces formed by the anion sublattice. The energy barrier to motion will be smaller for compounds containing large and polarizable (i.e. deformable) anions, such as iodine. However, this factor may not be as important as previously thought.

In the case of α-AgI [3, 4] and α-CuBr [6, 7], the cations preferentially occupy the tetrahedral cavities formed by the b.c.c. anion sublattice. Conduction between neighbouring tetrahedral interstices is believed to occur via the trigonal sites, rather than the octahedral ones (see figure 1). CuCl-III also shows preferential occupation of the tetrahedral sites, with marginal evidence (discussed in the previous section) for cations on trigonal positions. It is difficult to assign reliable values for the ionic radii of Cu^+ and Cl^- because CuCl has significant covalent character. However, some general geometric remarks can be made if we assume that cation sites adjacent to an occupied cation position are empty. This approach is justified, since the unit cell contains two Cu^+ distributed over a total of 42 available sites. With reference to figure 1, the octahedral cation coordination is somewhat distorted, with two anions at a distance $a/2$ and four at $a/\sqrt{2}$, whilst the tetrahedral and trigonal coordinations are both regular (four at $\sqrt{5}a/4$ and three at $\sqrt{18}a/8$, respectively). On the basis of minimum Cu^+–Cl^- distance, the interstitial interstices decrease in size in the order tetrahedral $\rightarrow$ trigonal $\rightarrow$ octahedral. However, if we use the average Cu^+–Cl^- distance as the criterion then the order becomes octahedral $\rightarrow$ tetrahedral $\rightarrow$ trigonal. Clearly, it is difficult to make unambiguous comments on the relative sizes of the interstitial cavities, though it is interesting to note that the cations reside in tetrahedral environments in the zinc-blende (phase II), wurtzite (phase I) and high-pressure (CuCl-IV) phases (see figure 2), though the coordination is somewhat distorted in the latter [15]. A pressure of $\sim$100 kbar is required to transform CuCl to the octahedrally coordinated rock-salt phase, CuCl-V [15].

Finally, it appears counter-intuitive that CuCl exhibits superionic behaviour at elevated, rather than ambient, pressure. The effect of hydrostatic pressure is to reduce the size of the gaps in the anion sublattice through which the cations migrate, or to induce phase transitions to more densely packed structures. In the case of CuCl, phase III is $\sim$5% more dense than the ambient pressure wurtzite phase at 683 K [5]. This implies that a body-centred-cubic anion sublattice (such as α-AgI and α-CuBr) is well suited to high cation mobility, presumably because there are six available tetrahedral interstices per cation. In comparison, only two tetrahedral holes per cation are found in face-centred-cubic (such as γ-CuCl) and hexagonal (β-CuCl) lattices. This hypothesis is also supported by the generally higher values of ionic conductivity observed in b.c.c.-based superionics [16].

5. Conclusions

Powder neutron diffraction studies have confirmed the presence of a solid phase in CuCl at elevated pressures and temperatures. The structure of CuCl-III comprises a disordered cation sublattice, with Cu^+ randomly distributed over the tetrahedral voids formed by a body-centred-cubic anion sublattice. This structural arrangement is also adopted by the ambient pressure superionic phases α-AgI [3, 4] and α-CuBr [6, 7] and appears highly favourable for unhindered cation mobility. The last member of the family of four tetrahedrally coordinated halides, CuI, differs because it adopts a face-centred anion array in its superionic α-phase. However, there is evidence of a further phase labelled CuI-VII, stable at pressures in excess of $\sim$10 kbar and temperatures in excess of $\sim$1050 K [11]. It would be interesting to know whether this phase is also a b.c.c.-based superionic.

In the wider context of structural studies of superionics it is clear that high-pressure investigations can provide valuable information. The presence of additional superionic phases at elevated p and T allows structural trends to be identified and the relative importance of factors such as crystal structure, unit-cell volume, ionic size and polarizability can be assessed. Such information also provides a stringent test for competing models for the superionic process. Future developments of the high-pressure–high-temperature device used in this work [13] are planned, to allow higher p- and T-ranges to be accessed and *in situ* measurements of the ionic conductivity during a neutron diffraction experiment.

Acknowledgment

The work presented in this paper forms part of a wider research project funded by the Engineering and Physical Sciences Research Council (reference P:AK:113 C2).

References

[1] Wyckoff R W G 1982 *Crystal Structures* vol 1 (Malabar, FL: Krieger)
[2] Merrill L 1977 *J. Phys. Chem. Ref. Data* **6** 1205
[3] Wright A F and Fender B E F 1977 *J. Phys. C: Solid State Phys.* **10** 2261
[4] Nield V M, Keen D A, Hayes W and McGreevy R L 1993 *Solid State Ion.* **66** 247
[5] Graneli B, Dahlborg U and Fischer P 1988 *Solid State Ion.* **28–30** 284
[6] Bührer W and Hälg W 1977 *Electrochim. Acta* **22** 701
[7] Nield V M, McGreevy R L, Keen D A and Hayes W 1994 *Physica* B **202** 159
[8] Keen D A and Hull S 1994 *J. Phys.: Condens. Matter* **6** 1637
[9] Boyce J B, Hayes T M and Mikkelsen J C Jr 1981 *Phys. Rev.* B **23** 2876 and references therein
[10] Jayaraman A, Newton R C and Kennedy G C 1962 *Proc. Int. Conf. on Industrial Diamonds (Paris)* p 297
[11] Rapoport E and Pistorius C W F T 1968 *Phys. Rev.* **172** 838
[12] Hull S, Smith R I, David W I F, Hannon A C, Mayers J and Cywinski R 1992 *Physica* B **180+181** 1000
[13] Hull S, Keen D A, Cooper T, Done R, Pike T, Fütterer K, Hayes W and Gardner N J G 1996 in preparation
[14] David W I F, Ibberson R M and Matthewman J C 1992 unpublished
[15] Hull S and Keen D A 1994 *Phys. Rev.* B **50** 5868
[16] Boyce J B and Huberman B A 1979 *Phys. Rep.* **51** 189